

Mixed Semiclassical Initial Value Representation Time-Averaging Propagator for Spectroscopic Calculations

Max Buchholz

*Institut für Theoretische Physik, Technische Universität Dresden, 01062 Dresden,
Germany and Max-Planck-Institut für Physik Komplexer Systeme,
Nöthnitzer Str. 38, 01187 Dresden, Germany*

Frank Grossmann

Institut für Theoretische Physik, Technische Universität Dresden, 01062 Dresden, Germany

Michele Ceotto

*Dipartimento di Chimica, Università degli Studi di Milano,
via C. Golgi 19, 20133 Milano, Italy**

Abstract

A mixed semiclassical initial value representation expression for spectroscopic calculations is derived. The formulation takes advantage of the time-averaging filtering and the hierarchical properties of different trajectory based propagation methods. A separable approximation is then introduced that greatly reduces (about an order of magnitude) the computational cost compared with a full Herman-Kluk time-averaging semiclassical calculation for the same systems. The expression is exact for the harmonic case and it is tested numerically for a Morse potential coupled to one or two additional harmonic degrees of freedom. Results are compared to full Herman-Kluk time-averaging calculations and exact quantum wavepacket propagations. We found the peak positions of the mixed semiclassical approximations to be always in very good agreement with full quantum calculations, while overtone peak intensities are lower with respect to the exact ones. Given the reduced computational effort required by this new mixed semiclassical approximation, we believe the present method to make spectroscopic calculations available for higher dimensional systems than accessible before.

* michele.ceotto@unimi.it

I. INTRODUCTION

Molecular spectra, and spectroscopic signals in general, contain all quantum mechanical information connected to molecular motion, even for increasingly complex systems. Most frequently, however, the full amount of information is not useful and not necessary. Actually, it would be convenient to be able to select with precision a certain amount of spectroscopic information that is related to a subset of degrees of freedom, which one is most interested in. In other words, since not all degrees of freedom are equally important, many relevant molecular properties of chemical systems can be rationalized in terms of few main degrees of freedom, usually called the “system”. These are coupled to an environment of many other degrees of freedom, the “bath”, which is not directly responsible for the physical properties in question.

In a time-dependent approach to spectroscopy, exact quantum mechanical methods to determine the dynamics of the complete dynamical system are inaccessible for most real-life applications. A common strategy therefore is to employ an accurate quantum propagator for the time-evolution of the system degrees of freedom and a lower accuracy propagation scheme for the bath ones. This should be done without enforcing any artificial and arbitrary decoupling between the system and the bath. Semiclassical Initial Values Representation (SC-IVR) molecular dynamics [1–4] is a valuable tool for exploiting this strategy, since it offers a hierarchy of semiclassical propagators at different levels of quantum accuracy. In the past, several groups have beaten this path in the search for a hybrid semiclassical propagator. For example, Zhang and Pollak, in their SC-IVR perturbative series method [5], treated the system variables with the Herman-Kluk (HK) prefactor [6] and the bath variables using a prefactor free propagation. This is obtained by forcing a unitary pre-exponential factor of the HK propagator, which is expensive to compute as the dimensionality of the problem increases [7]. Earlier, Ovchinnikov and Apkarian focused on condensed phase spectroscopy by using second- and zeroth order approximations in stationary phase of the exact quantum propagator, respectively the van Vleck and a prefactor-free van Vleck propagator in Initial Value Representation (vV-IVR) [8]. At about the same time, Sun and Miller introduced a mixed semiclassical-classical model, where the vV-IVR is either used in first or zeroth order approximation, according to the amount of quantum delocalization retained around each classical trajectory [9]. Also the Filinov smoothing can be used to tune the semiclassical propagator [10], as recently shown [11]. In 2006, one of us (FG) implemented a similar idea for the Gaussian dressed semiclassical dynamics of the HK propagator [12]. More specifically, Gaussian wave

packet propagation with the HK propagator is equivalent to a Thawed Gaussian wave packet dynamics (TGWD) [13] if the phase space integral is approximated to second order in the exponent around the phase space center of the wave packet (linearization of the classical trajectories) [14, 15]. If the transition from HK to TGWD is performed analytically only for a selected set of degrees of freedom, one obtains a semiclassical hybrid dynamics (SCHD) in the same spirit as described above. The HK propagator is quite accurate and definitely superior to a single trajectory TGWD, but computationally much more expensive for many degrees of freedom. However, the full HK propagator is not necessary to describe the dynamics for harmonic like modes, where the TGWD is already quite accurate[16–19]. The semiclassical hybrid propagation takes advantage of both methods when the system is treated at the level of HK and the bath with the TGWD.

For the pure HK propagator the method of time-averaging [20] has been shown to improve the numerical efficiency for the calculation of spectra, after the so-called separable approximation [21]. The goal in the following is to apply the time-averaging idea together with the SCHD propagation scheme to produce a mixed semiclassical time-averaging propagator for spectroscopic calculations.

The paper is organized in the following way. Section II recalls the time-averaging semiclassical method. Section III introduces a new mixed semiclassical propagator and Section IV presents a computationally cheap version of this propagator based on a separable approximation. In Section V results for the Caldeira-Leggett model Hamiltonian are presented and compared with exact quantum wave packet propagations. After a discussion of the results in Section V, Conclusions are drawn in Section VI.

II. THE TIME-AVERAGING SC-IVR METHOD FOR POWER SPECTRA CALCULATIONS

This paper focuses on spectroscopic calculations. More specifically, we want to calculate the power spectra components $I(E)$ of a given reference state $|\chi\rangle$ subject to the Hamiltonian \hat{H} ,

$$I(E) = \sum_i |\langle \chi | \psi_i \rangle|^2 \delta(E - E_i), \quad (1)$$

where E_i are the eigen-energies that we are interested in and $|\psi_i\rangle$ are the associated eigen-functions of the Hamiltonian. By representing the Dirac-delta in terms of a Fourier integral, Eq. (1) can be written as [22]

$$I(E) = \frac{1}{2\pi\hbar} \int_{-\infty}^{\infty} dt e^{iEt/\hbar} \langle \chi | e^{-i\hat{H}t/\hbar} | \chi \rangle \quad (2)$$

In semiclassical dynamics, the time evolution of Eq. (2) can be calculated using the HK propagator

$$e^{-i\hat{H}t/\hbar} = \frac{1}{(2\pi\hbar)^F} \int d\mathbf{p}(0) \int d\mathbf{q}(0) C_t(\mathbf{p}(0), \mathbf{q}(0)) \times e^{iS_t(\mathbf{p}(0), \mathbf{q}(0))/\hbar} |\mathbf{p}(t), \mathbf{q}(t)\rangle \langle \mathbf{p}(0), \mathbf{q}(0)|, \quad (3)$$

where $(\mathbf{p}(t), \mathbf{q}(t))$ is the set of $2F$ -dimensional classically-evolved phase space coordinates and S_t is the corresponding classical action. The integral representation of the propagator goes back to the Frozen Gaussian Approximation of Heller [23]. The pre-exponential factor

$$C_t(\mathbf{p}(0), \mathbf{q}(0)) = \sqrt{\det \left[\frac{1}{2} \left(\frac{\partial \mathbf{q}(t)}{\partial \mathbf{q}(0)} + \frac{\partial \mathbf{p}(t)}{\partial \mathbf{p}(0)} - i\hbar \gamma \frac{\partial \mathbf{q}(t)}{\partial \mathbf{p}(0)} + \frac{i}{\gamma \hbar} \frac{\partial \mathbf{p}(t)}{\partial \mathbf{q}(0)} \right) \right]} \quad (4)$$

takes into account second-order quantum delocalizations about the classical paths [1, 24, 26–37]. The prefactor in Eq. (4) is obtained if the initial state is represented in the coherent-state basis set [6, 25], which, for many degrees of freedom, is given by the direct product of one dimensional coherent states

$$\langle \mathbf{q} | \mathbf{p}(t), \mathbf{q}(t) \rangle = \prod_i \left(\frac{\gamma_i}{\pi} \right)^{F/4} \exp \left[-\frac{\gamma_i}{2} (q_i - q_i(t))^2 + \frac{i}{\hbar} p_i(t) (q_i - q_i(t)) \right], \quad (5)$$

where γ_i is fixed. For spectroscopic calculations, γ_i is conveniently set equal to the width of the harmonic oscillator approximation to the vibrational wave function for the i -th normal mode.

To accelerate the Monte Carlo phase space integration of Eq. (3), a time-averaging (TA) integral has been introduced [20, 21, 38]. Then, Eq. (2) becomes

$$I(E) = \frac{1}{(2\pi\hbar)^F} \int d\mathbf{p}(0) \int d\mathbf{q}(0) \frac{\text{Re}}{\pi\hbar T} \int_0^T dt_1 \int_{t_1}^T dt_2 C_{t_2}(\mathbf{p}(t_1), \mathbf{q}(t_1)) \times \langle \chi | \mathbf{p}(t_2), \mathbf{q}(t_2) \rangle e^{i(S_{t_2}(\mathbf{p}(0), \mathbf{q}(0)) + Et_2)/\hbar} \left[\langle \chi | \mathbf{p}(t_1), \mathbf{q}(t_1) \rangle e^{i(S_{t_1}(\mathbf{p}(0), \mathbf{q}(0)) + Et_1)/\hbar} \right]^*, \quad (6)$$

where the initial phase space point $(\mathbf{p}(0), \mathbf{q}(0))$ has been evolved to the Fourier integration time t_1 , respectively to the time averaging time t_2 , and T is the total simulation time. The computational effort of the double time variable integration can be alleviated by approximating the pre-exponential factor as $C_{t_2}(\mathbf{p}(t_1), \mathbf{q}(t_1)) \approx \exp[i(\phi(t_2) - \phi(t_1))/\hbar]$, where $\phi(t)/\hbar =$

phase $[C_t(\mathbf{p}(0), \mathbf{q}(0))]$. This is called the “separable approximation” and Eq. (6) becomes

$$I(E) = \frac{1}{(2\pi\hbar)^F} \frac{1}{2\pi\hbar T} \int d\mathbf{p}(0) \int d\mathbf{q}(0) \times \left| \int_0^T dt \langle \chi | \mathbf{p}(t), \mathbf{q}(t) \rangle e^{i[S_t(\mathbf{p}(0), \mathbf{q}(0)) + Et + \phi_t(\mathbf{p}(0), \mathbf{q}(0))]/\hbar} \right|^2 \quad (7)$$

in the separable approximation. The integral in Eq. (7) contains a single and positive-definite time integrand, which is more stable numerically than that one of Eq. (6). Furthermore, the numerical evaluation of (7) is quite accurate[21, 38] and much less computationally demanding than that of (6).

A recent implementation of Eqs. (6) and (7) is that of Ceotto et al., called “Multiple Coherent SC-IVR” (MC-SC-IVR) [38–45], where the reference state $|\chi\rangle = \sum_{i=1}^{N_{\text{states}}} |\mathbf{p}_{\text{eq}}^i, \mathbf{q}_{\text{eq}}^i\rangle$ is written as a combination of coherent states placed nearby the classical phase space points $(\mathbf{p}_{\text{eq}}^i, \mathbf{q}_{\text{eq}}^i)$, where \mathbf{q}_{eq}^i is an equilibrium position and \mathbf{p}_{eq}^i corresponds, in a harmonic fashion, to excited vibrational states, i.e. $(p_{i,\text{eq}})^2/2m = \hbar\omega_i(n+1/2)$. In this way, one can reduce the number of trajectories to a few “eigen-trajectories”, one for each coherent state location, corresponding to the harmonic sequence of eigenvalues. The Gaussian delocalization showed to alleviate the shortcomings of a global harmonic approximation, that one would perform if just a single trajectory was used, and to fully provide anharmonic effects. MC-SC-IVR has been successfully applied to gas phase spectra calculations of the H₂O molecule [38], and CO molecules chemisorbed on a Cu(100) surface using a pre-computed potential [42]. Using a direct *ab initio* approach, vibrational energies for CO₂ [38, 39], H₂CO [41] and the ammonia umbrella inversion [44], as well as CO₂ vibrational eigenfunctions [40], have been calculated. The MC-SC-IVR computational time is dramatically reduced when the method is implemented for GPU architectures [46].

III. A MIXED SEMICLASSICAL POWER SPECTRUM METHOD

The idea of the SCHD is based on a mixed semiclassical propagator approach. We partition the $2F$ phase space variables into $2F_{\text{hk}}$ for the system phase space and $2F_{\text{tg}}$ for the bath phase space. The HK level of accuracy is reserved for the system only, indicated by the subscript hk, whereas the bath phase space variables are treated on the thawed Gaussian level (subscript tg). The reference state is chosen as $|\chi\rangle = |\mathbf{p}_{\text{eq}}(0), \mathbf{q}_{\text{eq}}(0)\rangle$ as explained above, and the initial phase

space coordinate vectors are subdivided as

$$\mathbf{p}_{\text{eq}}(0) \equiv \begin{pmatrix} \mathbf{p}_{\text{eq, hk}}(0) \\ \mathbf{p}_{\text{eq, tg}}(0) \end{pmatrix}; \quad \mathbf{q}_{\text{eq}}(0) \equiv \begin{pmatrix} \mathbf{q}_{\text{eq, hk}}(0) \\ \mathbf{q}_{\text{eq, tg}}(0) \end{pmatrix} \quad (8)$$

where the bath starting coordinates are always assumed to be at the equilibrium positions. This phase space variable partitioning is motivated by considering that the TGWD exactly reproduces the full harmonic spectrum, as shown in Appendix VI. The partitioning should be well suited for a harmonic-like motion of the bath degrees of freedom.

Following [12], we approximate the evolution of the phase space coordinates in (8) at each time step as

$$\mathbf{q}(t) \equiv \begin{pmatrix} \mathbf{q}_{\text{hk}}(t) \\ \mathbf{q}_{\text{tg}}(t) \end{pmatrix} = \mathbf{q}_{\text{eq}}(t) + \mathbf{m}_{22}(t) \delta \mathbf{q}_{\text{tg}} + \mathbf{m}_{21}(t) \delta \mathbf{p}_{\text{tg}} \quad (9)$$

$$\mathbf{p}(t) \equiv \begin{pmatrix} \mathbf{p}_{\text{hk}}(t) \\ \mathbf{p}_{\text{tg}}(t) \end{pmatrix} = \mathbf{p}_{\text{eq}}(t) + \mathbf{m}_{12}(t) \delta \mathbf{q}_{\text{tg}} + \mathbf{m}_{11}(t) \delta \mathbf{p}_{\text{tg}} \quad (10)$$

where the trajectory coordinates are linearly expanded for the bath DOFs only. The matrices

$$\begin{aligned} \mathbf{m}_{11}(t) &= \frac{\partial \mathbf{p}_{\text{eq}}(t)}{\partial \mathbf{p}_{\text{eq, tg}}(0)}; & \mathbf{m}_{12}(t) &= \frac{\partial \mathbf{p}_{\text{eq}}(t)}{\partial \mathbf{q}_{\text{eq, tg}}(0)}; \\ \mathbf{m}_{21}(t) &= \frac{\partial \mathbf{q}_{\text{eq}}(t)}{\partial \mathbf{p}_{\text{eq, tg}}(0)}; & \mathbf{m}_{22}(t) &= \frac{\partial \mathbf{q}_{\text{eq}}(t)}{\partial \mathbf{q}_{\text{eq, tg}}(0)}; \end{aligned} \quad (11)$$

are non-square $F \times F_{\text{tg}}$ dimensional and the displacements

$$\begin{aligned} \delta \mathbf{p}_{\text{tg}} &= \mathbf{p}_{\text{tg}}(0) - \mathbf{p}_{\text{eq, tg}}(0) \\ \delta \mathbf{q}_{\text{tg}} &= \mathbf{q}_{\text{tg}}(0) - \mathbf{q}_{\text{eq, tg}}(0) \end{aligned} \quad (12)$$

are F_{tg} dimensional. To apply this approximation to Eq. (7), we express it as

$$\begin{aligned} I(E) &= \frac{1}{(2\pi\hbar)^F} \frac{1}{2\pi\hbar T} \int d\mathbf{p}(0) \int d\mathbf{q}(0) \\ &\times \left| \int_0^T dt e^{i(S_t(\mathbf{p}(0), \mathbf{q}(0)) + Et + \phi_t(\mathbf{p}(0), \mathbf{q}(0))/\hbar)} \right. \\ &\times \exp \left\{ -\frac{1}{4} (\mathbf{q}(t) - \mathbf{q}_{\text{eq}}(0))^T \boldsymbol{\gamma} (\mathbf{q}(t) - \mathbf{q}_{\text{eq}}(0)) \right\} \\ &\times \exp \left\{ -\frac{1}{4\hbar^2} (\mathbf{p}(t) - \mathbf{p}_{\text{eq}}(t))^T \boldsymbol{\gamma}^{-1} (\mathbf{p}(t) - \mathbf{p}_{\text{eq}}(t)) \right\} \\ &\times \exp \left\{ +\frac{i}{2\hbar} (\mathbf{q}_{\text{eq}}(0) - \mathbf{q}(t))^T (\mathbf{p}(t) + \mathbf{p}_{\text{eq}}(0)) \right\} \Big|^2 \end{aligned} \quad (13)$$

where the coherent reference state is explicitly written out.

We now express all quantities appearing in (13) in terms of the trajectory in Eqs. (9) and (10). The classical action becomes

$$\begin{aligned}
S_t(\mathbf{p}(0), \mathbf{q}(0)) = S_t(\mathbf{p}_{\text{hk}}(0), \mathbf{q}_{\text{hk}}(0), \mathbf{p}_{\text{eq, tg}}(0), \mathbf{q}_{\text{eq, tg}}(0)) \\
+ \mathbf{p}_{\text{eq}}^T(t) \mathbf{m}_{21}(t) \delta \mathbf{p}_{\text{tg}} + (\mathbf{p}_{\text{eq}}^T(t) \mathbf{m}_{22}(t) - \mathbf{p}_{\text{eq, 0, tg}}^T) \delta \mathbf{q}_{\text{tg}} \\
+ \frac{1}{2} \delta \mathbf{p}_{\text{tg}}^T \mathbf{m}_{11}^T(t) \mathbf{m}_{21}(t) \delta \mathbf{p}_{\text{tg}} + \frac{1}{2} \delta \mathbf{q}_{\text{tg}}^T \mathbf{m}_{12}^T(t) \mathbf{m}_{22}(t) \delta \mathbf{q}_{\text{tg}} \\
+ \delta \mathbf{q}_{\text{tg}}^T \mathbf{m}_{12}^T(t) \mathbf{m}_{21}(t) \delta \mathbf{p}_{\text{tg}}
\end{aligned} \tag{14}$$

up to the second order in fluctuations for the bath subspace[12]. In the same fashion, we insert (9) and (10) into the coherent states overlap, retain the terms up to the second order and obtain three approximated exponential terms. By inserting these terms and Eq. (14) into the power spectrum expression (13), we obtain the mixed semiclassical power spectrum approximation

$$\begin{aligned}
I(E) = \frac{1}{(2\pi\hbar)^F} \frac{1}{2\pi\hbar T} \int d\mathbf{p}(0) \int d\mathbf{q}(0) \left| \int_0^T dt e^{i[Et + \phi_t(\mathbf{p}(0), \mathbf{q}(0))]/\hbar} \right. \\
\times \exp \left\{ -\frac{1}{4} (\mathbf{q}_{\text{hk}}(t) - \mathbf{q}_{\text{hk}}(0))^T \gamma_{\text{hk}} (\mathbf{q}_{\text{hk}}(t) - \mathbf{q}_{\text{hk}}(0)) \right\} \\
\times \exp \left\{ -\frac{1}{4\hbar^2} (\mathbf{p}_{\text{hk}}(t) - \mathbf{p}_{\text{hk}}(0))^T \gamma_{\text{hk}}^{-1} (\mathbf{p}_{\text{hk}}(t) - \mathbf{p}_{\text{hk}}(0)) \right\} \\
\times \exp \left\{ +\frac{i}{2\hbar} (\mathbf{q}_{\text{hk}}(0) - \mathbf{q}_{\text{hk}}(t))^T (\mathbf{p}_{\text{hk}}(t) + \mathbf{p}_{\text{hk}}(0)) \right\} \\
\times \exp \left\{ -\left(\begin{pmatrix} \delta \mathbf{p}_{\text{tg}} \\ \delta \mathbf{q}_{\text{tg}} \end{pmatrix}^T \mathbf{A}(t) \begin{pmatrix} \delta \mathbf{p}_{\text{tg}} \\ \delta \mathbf{q}_{\text{tg}} \end{pmatrix} + \mathbf{b}^T \begin{pmatrix} \delta \mathbf{p}_{\text{tg}} \\ \delta \mathbf{q}_{\text{tg}} \end{pmatrix} + c_t \right) \right\} \Big|^2,
\end{aligned} \tag{15}$$

where we have introduced the $F_{\text{tg}} \times F_{\text{tg}}$ diagonal matrices γ_{tg} and the $F_{\text{hk}} \times F_{\text{hk}}$ diagonal matrices γ_{hk} comprising the respective width parameters. In the last exponential of (15), the terms have been collected according to the respective power of $\delta \mathbf{p}_{\text{tg}}$ and $\delta \mathbf{q}_{\text{tg}}$. The zeroth order terms are

$$\begin{aligned}
c_t = \frac{i}{\hbar} S_t(\mathbf{p}_{\text{hk}}(0), \mathbf{q}_{\text{hk}}(0), \mathbf{p}_{\text{eq, tg}}(0), \mathbf{q}_{\text{eq, tg}}(0)) \\
- \frac{1}{4} (\mathbf{q}_{\text{eq, tg}}(t) - \mathbf{q}_{\text{eq, tg}}(0))^T \gamma_{\text{tg}} (\mathbf{q}_{\text{eq, tg}}(t) - \mathbf{q}_{\text{eq, tg}}(0)) \\
- \frac{1}{4\hbar^2} (\mathbf{p}_{\text{eq, tg}}(t) - \mathbf{p}_{\text{eq, tg}}(0))^T \gamma_{\text{tg}}^{-1} (\mathbf{p}_{\text{eq, tg}}(t) - \mathbf{p}_{\text{eq, tg}}(0)) \\
+ \frac{i}{2\hbar} (\mathbf{q}_{\text{eq, tg}}(0) - \mathbf{q}_{\text{eq, tg}}(t))^T (\mathbf{p}_{\text{eq, tg}}(t) + \mathbf{p}_{\text{eq, tg}}(0))
\end{aligned} \tag{16}$$

and the coefficients of the second order terms are collected in the matrix $\mathbf{A}(t)$ composed of the

following $F_{\text{tg}} \times F_{\text{tg}}$ blocks

$$\begin{aligned} \mathbf{A}_{11}(t) &= \frac{1}{4} \mathbf{m}_{21}^T(t) \gamma \mathbf{m}_{21}(t) + \frac{1}{4\hbar^2} \mathbf{m}_{11}^T(t) \gamma^{-1} \mathbf{m}_{11}(t) \\ \mathbf{A}_{12}(t) &= \frac{1}{4} \mathbf{m}_{21}^T(t) \gamma \mathbf{m}_{22}(t) + \frac{1}{4\hbar^2} \mathbf{m}_{11}^T(t) \gamma^{-1} \mathbf{m}_{12}(t) \\ \mathbf{A}_{21}(t) &= \frac{1}{4} \mathbf{m}_{22}^T(t) \gamma \mathbf{m}_{21}(t) + \frac{1}{4\hbar^2} \mathbf{m}_{12}^T(t) \gamma^{-1} \mathbf{m}_{11}(t) + \frac{i}{2\hbar} \\ \mathbf{A}_{22}(t) &= \frac{1}{4} \mathbf{m}_{22}^T(t) \gamma \mathbf{m}_{22}(t) + \frac{1}{4\hbar^2} \mathbf{m}_{12}^T(t) \gamma^{-1} \mathbf{m}_{12}(t). \end{aligned} \quad (17)$$

The coefficients of the first order terms in $\delta \mathbf{p}_{\text{tg}}$ and $\delta \mathbf{q}_{\text{tg}}$ are collected in a $2F_{\text{tg}}$ dimensional vector of the type

$$\mathbf{b}_t \equiv \begin{pmatrix} \mathbf{b}_{1,t} \\ \mathbf{b}_{2,t} \end{pmatrix} \quad (18)$$

where

$$\mathbf{b}_{1,t}^T = -\frac{1}{2} (\mathbf{q}(t) - \mathbf{q}(0))^T \left[\gamma \mathbf{m}_{21}(t) + \frac{i}{\hbar} \mathbf{m}_{11}(t) \right] \quad (19)$$

$$\begin{aligned} & -\frac{1}{2\hbar^2} (\mathbf{p}(t) - \mathbf{p}(0))^T [\gamma^{-1} \mathbf{m}_{11}(t) - i\hbar \mathbf{m}_{21}(t)] \\ \mathbf{b}_{2,t}^T &= -\frac{1}{2} (\mathbf{q}(t) - \mathbf{q}(0))^T \left[\gamma \mathbf{m}_{22}(t) + \frac{i}{\hbar} \mathbf{m}_{12}(t) \right] \\ & -\frac{1}{2\hbar^2} (\mathbf{p}(t) - \mathbf{p}(0))^T [\gamma^{-1} \mathbf{m}_{12}(t) - i\hbar \mathbf{m}_{22}(t)] - \frac{i}{\hbar} \mathbf{p}_{\text{eq, tg}}^T. \end{aligned} \quad (20)$$

To carry out the Gaussian integration in $\delta \mathbf{p}_{\text{tg}}$ and $\delta \mathbf{q}_{\text{tg}}$ in (15), we first unravel the modulus squared, then change the coordinates in the bath subspace from the phase space ones to the displacement ones of (12) and obtain

$$\begin{aligned} I(E) &= \frac{1}{(2\pi\hbar)^F} \frac{\text{Re}}{\pi\hbar T} \int_0^T dt_1 \int_{t_1}^T dt_2 \int d\mathbf{p}_{\text{hk}}(0) \int d\mathbf{q}_{\text{hk}}(0) \\ & \times e^{i[E(t_1-t_2) + \phi_{t_1}(\mathbf{p}(0), \mathbf{q}(0)) - \phi_{t_2}(\mathbf{p}(0), \mathbf{q}(0))]/\hbar} \\ & \times \langle \mathbf{p}_{\text{eq, hk}}(0), \mathbf{q}_{\text{eq, hk}}(0) | \mathbf{p}(t_1), \mathbf{q}(t_1) \rangle \langle \mathbf{p}(t_2), \mathbf{q}(t_2) | \mathbf{p}_{\text{eq, hk}}(0), \mathbf{q}_{\text{eq, hk}}(0) \rangle \\ & \times \int d\delta \mathbf{p}_{\text{tg}}(0) \int d\delta \mathbf{q}_{\text{tg}}(0) \exp \left\{ - \begin{pmatrix} \delta \mathbf{p}_{\text{tg}} \\ \delta \mathbf{q}_{\text{tg}} \end{pmatrix}^T (\mathbf{A}(t_1) + \mathbf{A}^*(t_2)) \begin{pmatrix} \delta \mathbf{p}_{\text{tg}} \\ \delta \mathbf{q}_{\text{tg}} \end{pmatrix} \right\} \\ & \times \exp \left\{ (\mathbf{b}_{t_1} + \mathbf{b}_{t_2}^*)^T \begin{pmatrix} \delta \mathbf{p}_{\text{tg}} \\ \delta \mathbf{q}_{\text{tg}} \end{pmatrix} + c_{t_1} + c_{t_2}^* \right\}. \end{aligned} \quad (21)$$

Finally, we integrate over the bath displacements coordinates and obtain the present mixed semi-

classical approximation of (6)

$$\begin{aligned}
I(E) = & \frac{1}{(2\hbar)^F} \frac{1}{\pi^{F_{\text{hk}}}} \frac{\text{Re}}{\pi \hbar T} \int d\mathbf{p}_{\text{hk}}(0) \int d\mathbf{q}_{\text{hk}}(0) \int_0^T dt_1 \int_{t_1}^T dt_2 \\
& \times e^{i[E(t_1-t_2) + \phi_{t_1}(\mathbf{p}(0), \mathbf{q}(0)) - \phi_{t_2}(\mathbf{p}(0), \mathbf{q}(0))]/\hbar} \\
& \times \langle \mathbf{p}_{\text{eq, hk}}(0), \mathbf{q}_{\text{eq, hk}}(0) | \mathbf{p}(t_1), \mathbf{q}(t_1) \rangle \langle \mathbf{p}(t_2), \mathbf{q}(t_2) | \mathbf{p}_{\text{eq, hk}}(0), \mathbf{q}_{\text{eq, hk}}(0) \rangle \\
& \times \sqrt{\frac{1}{\det(\mathbf{A}(t_1) + \mathbf{A}^*(t_2))}} \\
& \times \exp \left\{ \frac{1}{4} (\mathbf{b}_{t_1} + \mathbf{b}_{t_2}^*)^T (\mathbf{A}(t_1) + \mathbf{A}^*(t_2))^{-1} (\mathbf{b}_{t_1} + \mathbf{b}_{t_2}^*) + c_{t_1} + c_{t_2}^* \right\}.
\end{aligned} \tag{22}$$

Eq. (22) keeps the system quantum evolution at the level of accuracy of a semiclassical Herman-Kluk simulation implying a Monte Carlo sampling over all the system coordinates and momenta. Instead, the bath coordinates and momenta are not sampled, and all initial conditions for the bath subspace trajectories are fixed at equilibrium. However, quantum effects are included for the bath dynamics by the thawed Gaussian quantum delocalization. We stress that only the semiclassical propagator is approximated by using the hybrid idea. The evolution of the underlying classical trajectories is still full dimensional and system and bath are naturally coupled. It should also be mentioned that due to the imaginary part of $\mathbf{A}(t)$ being time independent, the radicand of the square root in (22) is real, so no extra care has to be taken in computing this quantity.

IV. SEPARABLE APPROXIMATIONS FOR THE MIXED SEMICLASSICAL POWER SPECTRUM METHOD

The double time integration of (22) can be quite computationally demanding and the advantage of the approximated thawed Gaussian dynamics for the bath coordinates is diminished by this double integration. To recover a separable approximation of the type of the original time-averaging SC-IVR expression of (7) for the mixed semiclassical expression of Eq. (22), we approximate the exponential part as follows

$$\begin{aligned}
& \frac{1}{4} (\mathbf{b}_{t_1} + \mathbf{b}_{t_2}^*)^T (\mathbf{A}(t_1) + \mathbf{A}^*(t_2))^{-1} (\mathbf{b}_{t_1} + \mathbf{b}_{t_2}^*) \\
& \approx \frac{1}{4} \mathbf{b}_{\text{m}, t_1}^T (\mathbf{A}(t_1) + \mathbf{A}^*(t_1))^{-1} \mathbf{b}_{\text{m}, t_1} + \frac{1}{4} [\mathbf{b}_{\text{m}, t_2}^T (\mathbf{A}(t_2) + \mathbf{A}^*(t_2))^{-1} \mathbf{b}_{\text{m}, t_2}]^*,
\end{aligned} \tag{23}$$

while the other exponential terms are naturally separable. The modified vector $\mathbf{b}_{\text{m}, t}$ is defined as

$$\mathbf{b}_{\text{m}, t} = \begin{pmatrix} \mathbf{b}_{1, t} \\ \mathbf{b}_{2, t} + \frac{i}{\hbar} \mathbf{p}_{\text{tg}} \end{pmatrix} \tag{24}$$

The pre-exponential square root term is also not separable, and we approximate it in the fashion of a geometric average by

$$\frac{1}{\sqrt{\det(\mathbf{A}(t_1) + \mathbf{A}^*(t_2))}} \approx \left(\frac{1}{\det(\mathbf{A}(t_1) + \mathbf{A}^*(t_1))} \right)^{1/4} \left(\frac{1}{\det(\mathbf{A}(t_2) + \mathbf{A}^*(t_2))} \right)^{1/4} \quad (25)$$

Using Eq.s (23) and (25), the expression for the power spectrum is greatly simplified

$$\begin{aligned} I(E) = & \frac{1}{(2\hbar)^F} \frac{1}{\pi^{F_{\text{hk}}}} \frac{1}{2\pi\hbar T} \int d\mathbf{p}_{\text{hk}}(0) \int d\mathbf{q}_{\text{hk}}(0) \left| \int_0^T dt e^{i[Et + \phi_t(\mathbf{p}(0), \mathbf{q}(0))]/\hbar} \right. \\ & \times \langle \mathbf{p}_{\text{eq,hk}}(0), \mathbf{q}_{\text{eq,hk}}(0) | \mathbf{p}(t), \mathbf{q}(t) \rangle \frac{1}{[\det(\mathbf{A}(t) + \mathbf{A}^*(t))]^{1/4}} \\ & \left. \times \exp \left\{ \frac{1}{4} \mathbf{b}_{\text{m},t}^T (\mathbf{A}(t) + \mathbf{A}^*(t))^{-1} \mathbf{b}_{\text{m},t} + c_t \right\} \right|^2 \end{aligned} \quad (26)$$

and much less computationally demanding since only a single time-integration is now requested. Eq. (26) still retains the full dimensional classical evolution and the thawed Gaussian approximation for the bath degrees of freedom only. However, the time-averaging part of the thawed Gaussian dynamics is less accurate than that one in Eq. (22).

Appendix A shows how the TGWD is exact for the power spectrum calculations of the harmonic oscillator, including all vibrational levels. This level of accuracy is preserved by our approximation. We demonstrate that the peak positions of the spectrum are indeed reproduced correctly in Appendix B. This is very important since the harmonic contribution is often the main contribution for the potential energy surface of bound systems.

V. RESULTS AND DISCUSSION

To test the accuracy of the power spectrum expression of Eq. (26), we consider a model system of a Morse oscillator coupled bilinearly (the Caldeira-Leggett (CL) model [47]) to one, respectively two harmonic oscillators. We intentionally keep the number of the bath modes low, since in this way we have exact quantum wavepacket results available for comparison. The CL Hamiltonian in atomic units is

$$H = H_s + \sum_{i=1}^{F_{\text{bath}}} \left\{ \frac{p_i^2}{2} + \frac{1}{2} \left[\omega_i y_i + \frac{c_i}{\omega_i} (s - s_{\text{eq}}) \right]^2 \right\} \quad (27)$$

where s is the system variable and s_{eq} its equilibrium position, and y_i are the bath coordinates and the bath masses are unitary. We choose bath parameters corresponding to an Ohmic density with

exponential cutoff, where the normalization factor c_i/ω_i and a system-bath coupling strength η are defined as in [48].

The system Hamiltonian H_s is that of a Morse potential

$$V_s(r) = D_e \left(1 - e^{-\alpha(r-r_e)}\right)^2 \quad (28)$$

where $D_e = 0.057$ a.u., $r_e = 0$ a.u., and $\alpha = 0.983$ a.u.. The mass of the Morse oscillator has been set to $M_r = 1.165 \times 10^5$ a.u. and the Morse frequency is $\omega_s = 9.724 \times 10^{-4}$ a.u., in order to reproduce the vibration of the I_2 molecule.

We will look at two different effective coupling strengths $\eta_{\text{eff}} = \eta / (m_s \omega_s)$ and three different cutoff frequencies ω_c . Note that ω_c is identical with the bath frequency for the two dimensional case; in the three dimensional calculations there is one additional bath oscillator of lower frequency. In one case, we intentionally choose a bath frequency that is resonant with the Morse potential's harmonic approximation, and another that is much lower than ω_s , and a third one in between. In the resonant case, one might expect that the hybrid method is quite poor, because the system, which is anharmonic, might drive the harmonic bath into anharmonic dynamics, which is not accounted for by TGWD part of the mixed semiclassical propagator.

The initial conditions are chosen in harmonic approximation as $(p(0), q(0)) = (\sqrt{m_s \omega_s}, 0)$ for the system. Also the bath is initially at its equilibrium position with harmonic zero point kinetic energy. We use 10^4 trajectories for the two-dimensional, and 5×10^4 trajectories for the three-dimensional calculations. While this is enough to get the main peak positions correctly, tight convergence of the hk result needs more trajectories, as shown exemplary in Table I. The time step is $\Delta t = T_s/20$ (where $T_s = 2\pi/\omega_s$), and the total number of (semiclassical) time steps is 2^{14} , except for Eq. (22) where we use only 2^{13} steps because we have to do two time integrations in that case. The reference quantum calculations are performed with the WavePacket software [49].

For a better comparability between spectra, we always subtract the uncoupled bath ground state energy in our plots, i. e.,

$$E_{\text{plot}} = E - \sum_{i=0}^{F_{\text{bath}}} \omega_i / 2. \quad (29)$$

Figure 1 shows the power spectra comparison for the two-dimensional simulations. For each plot, exact quantum wavepacket propagation is compared with the HK SC-IVR calculations at different levels of approximation. The “hk” label is for the Herman-Kluk SC-IVR propagator, the

	TA HK sep (7)	TA mixed (22)	TA mixed-sep (26)
trajectories	2×10^5	1×10^4	1×10^4
time steps	2^{14}	2^{13}	2^{14}
computational time	10 hours	33 hours	40 min

Table I. Number of trajectories and computational times needed for tight convergence of spectrum of a Morse oscillator coupled to 1 bath oscillator with $\eta_{\text{eff}} = 0.2$ and $\omega_{\text{bath}} = \omega_s/10$. All propagation times from single CPU calculations on a standard desktop computer.

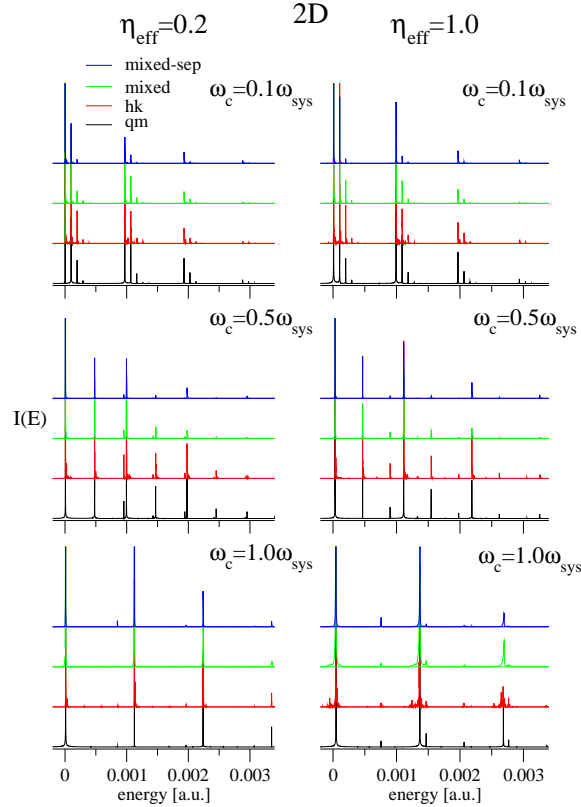


Figure 1. Two dimensional power spectra calculation at different level of semiclassical accuracy for different cutting frequency and bath friction values.

“mixed” is for Eq. (22) and the “mixed-sep” is for Eq. (26). To better appreciate the different levels of approximation, the results should be read in a hierarchical order by comparing the “mixed-sep” with the “mixed”, the “mixed” with the “hk” and the “hk” with the exact “qm”. It is quite surprising that independently of the coupling and of the system frequency, the separable approximation of Eq. (26), labeled “mixed-sep”, faithfully reproduces the spectral profile of the original approximation of Eq. (22), the “mixed” one. Peaks locations are also well reproduced by the “mixed” approximation with respect to the original “hk” one. However, the peak intensities are not well reproduced in the different approximations. Thus, the approximations described in Sections III and IV are suitable for locating the vibrational eigenvalues but it introduces some inaccuracy in the spectral intensities. Finally, the difference between the “hk” spectrum and the exact one are only for peak intensities and the different time propagation. In fact, the “hk” is employing long simulation times to exploit the time-averaging filter, while the quantum wave packet simulations are stopped at some computationally feasible time. All three cases show a blueshift of the system frequency (very clear in the middle panel) and a redshift of the bath frequency. For the stronger coupling, the blueshift tendency of the system is enhanced.

We now turn to the three-dimensional calculations shown in Fig. 2. Here, the spectroscopic features are much more complex and the simulation is quite more challenging than the previous one. Nevertheless, the “mixed” approximation is able to reproduce the “hk” results quite faithfully, since the peak positions are correct both in the resonant and off-resonance case. The most severe “mixed-sep” approximation is also reproducing both the “hk” and “mixed” results, even if it introduces some inaccuracy in the peak intensity and a few highly excited overtones are missing. Also in three dimensions, for the resonant case $\omega_c = \omega_s$, the resonant bath frequencies are strongly red shifted, while the blue shift of the system is further enhanced.

Considering the drastic computational effort reduction introduced by the Gaussian integration in Eq. (22), where a phase space integral is approximated by a single phase space trajectory, we think that the results in Figs (1) and (2) are quite satisfying. Even when the coupling between the system and the bath is resonant, the peak position is still quite accurate. The main drawback of the approximations “mixed” and “mixed-sep” is represented by the loss of intensity for some peaks. However, for complex systems this limitation could help for a better peak interpretation because the “mixed-sep” approximation mainly suppresses bath excitations in the spectrum, as we show in Appendix B.

On one hand, the “mixed” approximation is more computational expensive per trajectory than

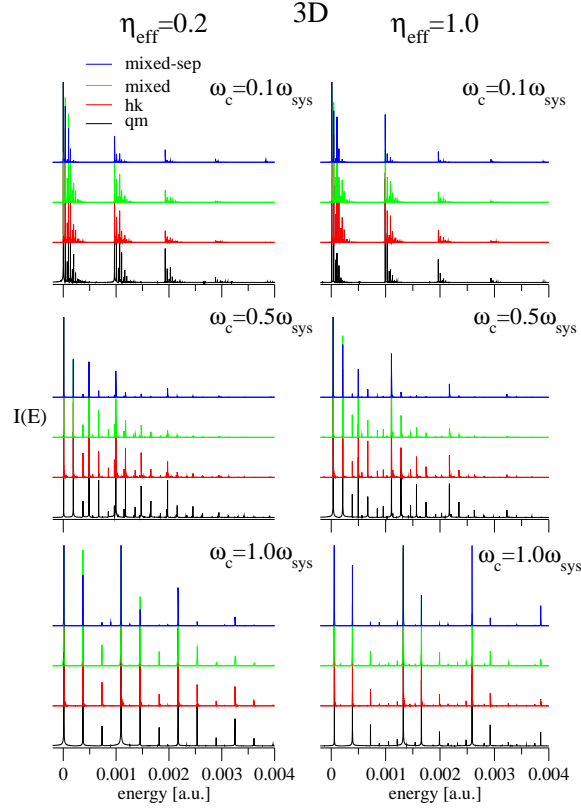


Figure 2. As in Fig.(1), but for three dimensional calculations.

the time averaged HK calculation because of the double time-integration. On the other hand, the number of trajectories needed for converging the phase space integral is reduced with respect to the full dimensional HK integration, because the integration is limited to the system's phase space. Table 1 shows that the “hk” calculation might still be faster than the full “mixed” one in spite of the reduction in the number of trajectories needed for convergence because of the unfavorable scaling of the “mixed” approximation with the number of time steps and because the calculation of the classical trajectories does not take much time in this example. For a realistic problem where the potential is not given analytically and the trajectory is simulated on-the-fly [38, 39, 41, 43, 44], the trajectory calculation will take much longer and make the “mixed” approach the more efficient one. The “mixed-sep” approximation, on the other hand, combines the single time integration of “hk” with the reduced number of trajectories, which results in an impressive speedup of the computations, as shown in Table 1. The inaccuracy that comes with this additional approximation is only in peak intensity, but not peak position, as discussed before.

VI. CONCLUSIONS

We have developed a new semiclassical method for the calculation of vibrational spectra of molecular systems that is based on the combination of the time-averaging idea with the semiclassical hybrid methodology. After partitioning the phase space variables into system and bath ones, we could apply a lower accuracy semiclassical propagation scheme based on a thawed Gaussian approximation to the bath degrees of freedom only, while preserving the full HK semiclassical propagator accuracy for the system time evolution. The resulting expression of the power spectrum intensity of Eq. (22) was then approximated to further reduce the computational effort. In this way, the separable approximation, that is at the heart of the time-averaging method, was implemented and lead to the final working formula, given in Eq. (26). In the harmonic case, this additional approximation has been shown to give identical peak positions in the spectrum, as can be seen by comparing the results in Appendix A and Appendix B. Numerical examples have been shown for a Morse oscillator coupled to one or two harmonic oscillators with different frequencies and coupling strengths. Even in the case of only one additional harmonic degree of freedom, compared to full Herman-Kluk time-averaging results, the numerical effort was shown to be reduced by more than an order of magnitude. Considering different system-bath couplings and including the resonant scenario, we found peak positions to be always in very good agreement with full quantum calculations, that are still feasible in the cases considered. In the future, we are planning to apply this semiclassical method to more realistic systems, where the harmonic bath is replaced by a realistic solvent, such as rare gas matrices [50, 51] or even water molecules.

ACKNOWLEDGEMENT

Michele Ceotto acknowledges support from the European Research Council (ERC) under the European Union’s Horizon 2020 research and innovation programme (grant agreement No [647107] – SEMICOMPLEX – ERC-2014-CoG). M.C. acknowledges also the CINECA and the Regione Lombardia award under the LISA initiative (grant SURGREEN) for the availability of high performance computing resources and the Chemistry Department of the University of Milan for funding through the Development Plan of Athenaeum grant – line B1 (UNIAGI 17777). FG gratefully acknowledges financial support from the Deutsche Forschungsgemeinschaft through Grant No. GR 1210/4-2.

APPENDIX A: THE HARMONIC SPECTRUM USING A THAWED GAUSSIAN WAVEPACKET

In this appendix, we show that the thawed Gaussian approximation (TGA) as an exact solution of the time-dependent Schrödinger equation for the harmonic oscillator leads to the exact harmonic spectrum. The wavepacket in the TGA [13] is written as the coherent state

$$\psi(x, t) = \left(\frac{\gamma_0}{\pi}\right)^{1/4} \exp \left\{ -\frac{\gamma_t}{2} (x - q_t)^2 + \frac{i}{\hbar} p_t (x - q_t) + \frac{i}{\hbar} \delta_t \right\}, \quad (30)$$

where the parameters γ_t and δ_t evolve with time according to the differential equations

$$-i\hbar\dot{\gamma}_t = -\frac{\hbar^2}{m}\gamma_t^2 + \frac{d^2}{dq_t^2} V(q_t, t) \quad (31)$$

$$\dot{\delta}_t = \frac{p_t^2}{2m} - V(q_t, t) - \frac{\hbar^2}{2m}\gamma_t. \quad (32)$$

For the harmonic oscillator motion where the potential is $V(q_t) = m\omega^2 q_t^2/2$, (31) and (32) become

$$-i\hbar\dot{\gamma}_t = -\frac{\hbar^2}{m}\gamma_t^2 + m\omega^2 \quad (33)$$

$$\dot{\delta}_t = S_t(p_0, q_0) - \frac{\hbar\omega}{2}t, \quad (34)$$

and $\gamma(t)$ is constant for the arbitrary and convenient choice of $\gamma(0) = m\omega/\hbar$. In this case, (30) becomes

$$\psi(x, t) = \left(\frac{\gamma_0}{\pi}\right)^{1/4} \exp \left\{ -\frac{\gamma_0}{2} (x - q_t)^2 + \frac{i}{\hbar} p_t (x - q_t) + \frac{i}{\hbar} S_t - \frac{i}{\hbar} \left(\frac{\hbar\omega}{2}\right) t \right\}. \quad (35)$$

The power spectrum is thus given by

$$\begin{aligned} I(E) &= \frac{1}{2\pi\hbar} \int_{-\infty}^{+\infty} dt e^{iEt/\hbar} \langle \psi(0) | \psi(t) \rangle \\ &= \frac{1}{2\pi\hbar} \int_{-\infty}^{+\infty} dt e^{iEt/\hbar} \int_{-\infty}^{+\infty} \psi^*(x, 0) \psi(x, t) dx \\ &= \frac{1}{2\pi\hbar} \int_{-\infty}^{+\infty} dt \exp \left\{ \frac{i}{\hbar} \left(E - \frac{\hbar\omega}{2} \right) t \right\} \\ &\quad \times \exp \left\{ -\frac{\gamma_0}{4} (q_t - q_0)^2 - \frac{1}{4\hbar^2\gamma_0} (p_t - p_0)^2 + \frac{i}{2\hbar} (q_0 p_t - q_t p_0) \right\}. \end{aligned} \quad (36)$$

After inserting the harmonic oscillator solutions

$$p_t = p_0 \cos \omega t - m\omega q_0 \sin \omega t \quad (37)$$

$$q_t = q_0 \cos \omega t + \frac{p_0}{m\omega} \sin \omega t, \quad (38)$$

choosing $\gamma_0 = m\omega/\hbar$ and doing a power series expansion of the second part of the exponential, the time integration in (36) can be done analytically to yield

$$I(E) = \frac{1}{2\pi\hbar} \int_{-\infty}^{\infty} dt \exp \left\{ \frac{i}{\hbar} \left[\left(E - \frac{\hbar\omega}{2} \right) t \right] + \frac{m\omega}{2\hbar} \left(\frac{p_0^2}{m^2\omega^2} + q_0^2 \right) (e^{-i\omega t} - 1) \right\} \quad (39)$$

$$= \exp \left\{ -\frac{m\omega}{2\hbar} q_0^2 - \frac{1}{2m\omega\hbar} p_0^2 \right\} \quad (40)$$

$$\times \sum_{k=0}^{+\infty} \frac{1}{2^k k!} \left(\frac{m\omega}{\hbar} q_0^2 + \frac{p_0^2}{m\omega\hbar} \right)^k \frac{1}{2\pi\hbar} \int_{-\infty}^{\infty} dt \exp \left\{ \frac{i}{\hbar} \left[\left(E - \frac{\hbar\omega}{2} - \hbar\omega k \right) t \right] \right\}$$

$$= \exp \left\{ -\frac{m\omega q_0^2}{2\hbar} - \frac{p_0^2}{2m\omega\hbar} \right\} \sum_{k=0}^{+\infty} \frac{1}{2^k k!} \left(\frac{m\omega q_0^2}{\hbar} + \frac{p_0^2}{m\omega\hbar} \right)^k \delta \left(E - \hbar\omega \left(k + \frac{1}{2} \right) \right), \quad (41)$$

which is the full harmonic spectrum, i.e. all vibrational levels are exactly reproduced.

APPENDIX B: THE HARMONIC SPECTRUM FROM THE HYBRID EXPRESSIONS

We demonstrate in this appendix how the approximations of the TG part leading from the original mixed semiclassical expression (22) to the simplified formula (26) affect the harmonic oscillator spectrum. In order to do so, we first go through the basic steps of calculating the spectrum (41) from Eq. (22). To keep it simple, we show this for one harmonic oscillator DOF that is treated with the TGA. The expression for the spectrum then emerges as a limiting case of Eq. (22) and reads

$$I(E) = \frac{1}{2\hbar} \frac{\text{Re}}{\pi\hbar T} \int_0^T dt_1 \int_{t_1}^T dt_2 e^{i[E(t_1-t_2) + \phi_{t_1}(p_0, q_0) - \phi_{t_2}(p_0, q_0)]/\hbar}$$

$$\times \sqrt{\frac{1}{\det(\mathbf{A}_{t_1} + \mathbf{A}_{t_2}^*)}} \exp \left\{ \frac{1}{4} (\mathbf{b}_{t_1} + \mathbf{b}_{t_2}^*)^T (\mathbf{A}_{t_1} + \mathbf{A}_{t_2}^*)^{-1} (\mathbf{b}_{t_1} + \mathbf{b}_{t_2}^*) + c_{t_1} + c_{t_2}^* \right\} \quad (42)$$

Using p_t and q_t from (37) and (38) and calculating the respective derivatives, the matrix \mathbf{A}_t from equation (17) becomes a constant in time

$$\mathbf{A} = \begin{pmatrix} 1/(4m\omega\hbar) & i/(4\hbar) \\ i/(4\hbar) & m\omega/(4\hbar) \end{pmatrix} \quad (43)$$

and the determinant from the prefactor is

$$\det(\mathbf{A}_{t_1} + \mathbf{A}_{t_2}^*) = \frac{1}{4\hbar^2}. \quad (44)$$

The vector \mathbf{b}_t , defined in (18), (19), and (20), has components

$$b_{1,t} = \frac{1}{2\hbar} (e^{-i\omega t} - 1) \left(\frac{p_0}{m\omega} + iq_0 \right) \quad (45)$$

$$b_{2,t} = -i \frac{m\omega}{2\hbar} (e^{-i\omega t} - 1) \left(\frac{p_0}{m\omega} + iq_0 \right) - \frac{i}{\hbar} p_0, \quad (46)$$

making the first term of the exponent in (42)

$$\frac{1}{4} (\mathbf{b}_{t_1} + \mathbf{b}_{t_2}^*)^T (\mathbf{A}_{t_1} + \mathbf{A}_{t_2}^*)^{-1} (\mathbf{b}_{t_1} + \mathbf{b}_{t_2}^*) = \frac{m\omega}{2\hbar} \left(\frac{p_0^2}{m^2\omega^2} + q_0^2 \right) \times (\mathbf{e}^{i\omega(t_2-t_1)} - \mathbf{e}^{-i\omega t_1} - \mathbf{e}^{i\omega t_2} + 1). \quad (47)$$

With the harmonic oscillator action

$$S_t = \left(\frac{p_0^2}{2m\omega} - \frac{1}{2}m\omega q_0^2 \right) \cos \omega t \sin \omega t - p_0 q_0 \sin^2 \omega t, \quad (48)$$

the scalar c_t from equation (16) is

$$c_t = \frac{m\omega}{2\hbar} \left(\frac{p_0^2}{m^2\omega^2} + q_0^2 \right) (\mathbf{e}^{-i\omega t} - 1). \quad (49)$$

Adding $c_{t_1} + c_{t_2}^*$ to (47), the total exponent in (42) is found to be

$$\frac{1}{4} (\mathbf{b}_{t_1} + \mathbf{b}_{t_2}^*)^T (\mathbf{A}_{t_1} + \mathbf{A}_{t_2}^*)^{-1} (\mathbf{b}_{t_1} + \mathbf{b}_{t_2}^*) + c_{t_1} + c_{t_2}^* = \frac{m\omega}{2\hbar} \left(\frac{p_0^2}{m^2\omega^2} + q_0^2 \right) \times (\mathbf{e}^{i\omega(t_2-t_1)} - 1). \quad (50)$$

Taking into account the phase of the prefactor $\phi(t) = -\hbar\omega t/2$ for the harmonic oscillator, the total expression for the spectrum takes the form

$$I(E) = \frac{\text{Re}}{\pi\hbar T} \int_0^T dt_1 \int_{t_1}^T dt_2 \exp \left\{ \frac{i}{\hbar} \left[E(t_1 - t_2) - \frac{\hbar\omega}{2} (t_1 - t_2) \right] \right\} \quad (51)$$

$$\times \exp \left\{ \frac{m\omega}{2\hbar} \left(\frac{p_0^2}{m^2\omega^2} + q_0^2 \right) (\mathbf{e}^{-i\omega(t_1-t_2)} - 1) \right\}. \quad (52)$$

Changing variables to $\tau \equiv t_2 - t_1$ yields after integration over $\tau_2 = t_1$

$$I(E) = \frac{\text{Re}}{\pi\hbar T} \int_0^T d\tau \exp \left\{ -\frac{i}{\hbar} \left[\left(E - \frac{\hbar\omega}{2} \right) \tau \right] + \frac{m\omega}{2\hbar} \left(\frac{p_0^2}{m^2\omega^2} + q_0^2 \right) (\mathbf{e}^{i\omega\tau} - 1) \right\}; \quad (53)$$

a series expansion of the second part of the exponent and another integration in the limit $T \rightarrow \infty$ reproduces (39).

Second, we consider the simplified hybrid approximation (26), which has the 1D TGA form

$$I(E) = \frac{1}{2\hbar} \frac{1}{2\pi\hbar T} \left| \int_0^T dt \mathbf{e}^{i[E t + \phi_t(p_0, q_0)]/\hbar} \times \frac{1}{[\det(\mathbf{A}_t + \mathbf{A}_t^*)]^{1/4}} \exp \left\{ \frac{1}{4} \mathbf{b}_{m,t}^T (\mathbf{A}_t + \mathbf{A}_t^*)^{-1} \mathbf{b}_{m,t} + c_t \right\} \right|^2. \quad (54)$$

The prefactor phase ϕ_t and scalar term in the exponent c_t obviously stay the same as in the full expression. Due to its time independence for the harmonic oscillator, the terms containing \mathbf{A}_t do not change either. This makes the approximation of the determinant (25) an exact identity. Comparing

(49), (53) and (54), we see that c_t is the only contribution we need for the exponent. Consequently, the modified vector $\mathbf{b}_{m,t}$, where the second component no longer contains the constant imaginary part,

$$b_{m,2,t}^T = -i \frac{m\omega}{2\hbar} (e^{-i\omega t} - 1) \left(\frac{p_0}{m\omega} + iq_0 \right), \quad (55)$$

is designed such that the contributions from the two components of $\mathbf{b}_{m,t}$ in the exponent cancel each other,

$$\frac{1}{4} \mathbf{b}_{m,t}^T (\mathbf{A}_t + \mathbf{A}_t^*)^{-1} \mathbf{b}_{m,t} = 0, \quad (56)$$

and the power spectrum resulting from these approximations

$$I(E) = \frac{1}{2\pi\hbar T} \left| \int_0^T dt \exp \left\{ \frac{i}{\hbar} \left(Et - \frac{\hbar\omega}{2} t \right) + \frac{m\omega}{2\hbar} \left(\frac{p_0^2}{m^2\omega^2} + q_0^2 \right) (e^{-i\omega t} - 1) \right\} \right|^2 \quad (57)$$

has a time integrand that is identical to the one in the full expression from Eq. (53). After a series expansion of the exponential as before, unfolding the modulus into the double integral $2\text{Re} \int_0^T dt_1 \int_{t_1}^T dt_2$ and changing variables as suggested above, the result after time integration is

$$I(E) = \exp \left\{ -\frac{m\omega q_0^2}{\hbar} - \frac{p_0^2}{m\omega\hbar} \right\} \sum_{k=0}^{+\infty} \frac{1}{(k!)^2} \left(\frac{m\omega q_0^2}{2\hbar} + \frac{p_0^2}{2m\omega\hbar} \right)^{2k} \delta \left(E - \hbar\omega \left(k + \frac{1}{2} \right) \right) \quad (58)$$

All harmonic oscillator peaks are placed at the right positions. Only the relative peak weight is the squared value compared to the correct result, thus damping peaks from higher (bath) excitations.

-
- [1] (a) W. H. Miller, J. Chem. Phys. **53**, 3578 (1970); (b) *ibidem* **53**, 1949 (1970); (c) W. H. Miller, J. Phys. Chem. A **105**, 2942 (2001).
 - [2] (a) E. J. Heller, J. Chem. Phys. **62**, 1544 (1975); (b) *ibidem* **75**, 2923 (1981); (c) *ibidem* **94**, 2723 (1991).
 - [3] W. H. Miller, Proc. Natl. Acad. Sci. U.S.A. **102**, 6660 (2005).
 - [4] K. G. Kay, Annu. Rev. Phys. Chem. **56**, 255 (2005).
 - [5] S. S. Zhang and E. Pollak, J. Chem. Phys. **121**, 3384 (2004).
 - [6] M. F. Herman, J. Chem. Phys. **85**, 2069 (1986); E. Kluk, M. F. Herman and H. L. Davis, J. Chem. Phys. **84**, 326 (1986).
 - [7] S. Zhang and E. Pollak, J. Chem. Theory Comput. **1**, 345 (2005).

- [8] M. Ovchinnikov and V. A. Apkarian, J. Chem. Phys. 105 (23), 10312 (1996); *ibidem* 106 (13), 5775 (1997); *ibidem* 108 (6), 2277 (1998).
- [9] X. Sun and W. H. Miller, J. Chem. Phys. **130**106 (3), 916 (1997).
- [10] M. Thoss, H. Wang and W. H. Miller, J. Chem. Phys. **114**, 9220 (2001)
- [11] S. V. Antipov, Z. Ye, and N. Ananth, J. Chem. Phys. **142**, 184102 (2015)
- [12] F. Grossmann, J. Chem. Phys. **125**, 014111 (2006).
- [13] E. J. Heller, J. Chem. Phys. **62**, 1544 (1975).
- [14] F. Grossmann, Comments At. Mol. Phys. **34**, 141 (1999).
- [15] S. A. Deshpande, G. S. Ezra, J. Phys. A 39, 5067 (2006).
- [16] M. Wehrle, M. Sulc, J. Vanicek, J. Chem. Phys. **140**, 244114 (2014)
- [17] M. Wehrle, S. Oberli, J. Vanicek, J. Phys. Chem A **119**, 5685 (2015)
- [18] S. Miroslav and J. Vanicek, Molecular Physics **110**, 945 (2012)
- [19] R. Conte and E. Pollak, Phys. Rev. E **81**, 036704 (2010).
- [20] Y. Elran and K. G. Kay, J. Chem. Phys. **110**, 3653 (1999); *ibidem* **110**, 8912 (1999).
- [21] A. L. Kaledin and W. H. Miller, J. Chem. Phys. **118**, 7174 (2003); A. L. Kaledin and W. H. Miller, J. Chem. Phys. **119**, 3078 (2003).
- [22] E. J. Heller, Acc. Chem. Res. **14**, 368 (1981)
- [23] E. J. Heller, J. Chem. Phys. 75, 2923 (1981).
- [24] (a) K. G. Kay, J. Chem. Phys. **100**, 4377 (1994); (b) *ibidem* **100**, 4432 (1994).; (c) K. G. Kay, J. Chem. Phys. **101**, 2250 (1994).
- [25] F. Grossmann and A. L. Xavier, Phys. Lett. 243, 243 (1998).
- [26] (a) A. R. Walton, D. E. Manolopoulos, Mol. Phys. **87**, 961 (1996); (b) A. R. Walton, D. E. Manolopoulos, Chem. Phys. Lett. **244**, 448 (1995); (c) M. L. Brewer, J. S. Hulme, D. E. Manolopoulos, J. Chem. Phys. **106**, 4832 (1997).
- [27] S. Bonella, D. Montemayor , and D. F. Coker, Proc. Natl. Am. Soc. **102**, 6715 (2005).
- [28] (a) H. Ushiyama and K. Takatsuka, J. Chem. Phys. **122**, 224112 (2005); (b) S. Takahashi and K. Takatsuka, J. Chem. Phys. **127**, 084112 (2007).
- [29] B. B. Issack and P. N. Roy, J. Chem. Phys. **127**, 054105 (2007).
- [30] (a) E. Pollak and E. Martin-Fierro, J. Chem. Phys. **126**, 164107 (2007); (b) E. Martin-Fierro and E. Pollak, J. Chem. Phys. **125**, 164104 (2006).
- [31] (a) H. Wang, X. Sun, and W. H. Miller, J. Chem. Phys. **108**, 9726 (1988); (b) T. Yamamoto, H. Wang,

- and W. H. Miller, J. Chem. Phys. **116**, 7335 (2002); (c) T. Yamamoto, W. H. Miller, J. Chem. Phys. **118**, 2135 (2003).
- [32] G. Tao and W. H. Miller, J. Chem. Phys. **135**, 024104 (2011); *ibidem* **137**, 124105 (2012); G. Tao and W. H. Miller, J. Chem. Phys. **137**, 124105 (2012)
- [33] S. Y. Y. Wong, D. M. Benoit, M. Lewerenz, A. Brown, and P.-N. Roy, J. Chem. Phys. **134**, 094110 (2011)
- [34] N. T. Maitra, J. Chem. Phys. **112**, 531 (2000).
- [35] J. Liu, Int. J. of Quantum Chemistry, **115** (11), 657 (2015)
- [36] G. Tao, J. Phys. Chem. A **117**, 5821–5825 (2013)
- [37] J.C. Burant and V.S. Batista, J. Chem. Phys. **116**, 2748–2756 (2002)
- [38] M. Ceotto, S. Atahan, G. F. Tantardini, and A. Aspuru-Guzik, J. Chem. Phys. **130**, 234113, (2009).
- [39] M. Ceotto, S. Atahan, S. Shim, G. F. Tantardini, and A. Aspuru-Guzik, Phys. Chem. Chem. Phys. **11**, 3861 (2009).
- [40] M. Ceotto, S. Valleau, G. F. Tantardini, and A. Aspuru-Guzik, J. Chem Phys. **134**, 234103 (2011).
- [41] M. Ceotto, G. F. Tantardini, and A. Aspuru-Guzik, J. Chem. Phys. **135**, 214108 (2011).
- [42] M. Ceotto, D. dell’Angelo, and G. F. Tantardini, J. Chem. Phys. **133**, 054701 (2010).
- [43] M. Ceotto, Y. Zhuang, and W. L. Hase, J. Chem. Phys. **138**, 054116 (2013).
- [44] R. Conte, A. Aspuru-Guzik, and M. Ceotto, *J. Phys. Chem. Lett.* **4**, 3407 (2013)
- [45] Y. Zhuang, M. R. Siebert, W. L. Hase, K. G. Kay, and M. Ceotto, J. Chem. Theory and Comput **9**, 54 (2013)
- [46] D. Tamascelli, F. S. Dambrosio, R. Conte, and M. Ceotto, J. Chem. Phys. **140**, 174109 (2014)
- [47] A. O. Cladeira and A. J. Leggett, Physica A **121**, 587 (1983)
- [48] C. Goletz, and F. Grossmann, J. Chem. Phys. **130**, 244107 (2009)
- [49] B. Schmidt and U. Lorenz, WavePacket 4.7.3, available via <http://sourceforge.net/projects/wavepacket/> (2011)
- [50] M. Buchholz, C. Goletz, F. Grossmann, B. Schmidt, J. Heyda, and P. Jungwirth, J. Phys. Chem. A, **116**, 11199 (2012)
- [51] Z. Bihary, R. B. Gerber, and V. A. Apkarian, J. Chem. Phys. **115**, 2695 (2001)